Section 8

Development of and advances in ocean, sea-ice, and wave modelling and data assimilation.

Improvement in JMA's Ocean Data Assimilation and Prediction System for the Seas Around Japan (JPN system)

HIRABARA Mikitoshi[1], ASAI Hiroaki[1] and USUI Norihisa[2]
1: Numerical Prediction Division, Japan Meteorological Agency
2: Meteorological Research Institute, Japan Meteorological Agency
E-mail: m.hirabara@met.kishou.go.jp

1. Introduction

Since October 2020, JMA has operated an ocean data assimilation and prediction system (known as the JPN system) for the seas around Japan to support analysis and prediction of major currents (such as the Kuroshio), mesoscale eddies, high tides caused by oceanic conditions, rapid coastal currents, and sea ice conditions (Sakamoto et al. 2019; Hirose et al. 2019). The JPN system consists of an analysis part and a prediction part. The analysis part incorporates an eddy-resolving North Pacific model with reduced grid configuration (NPR) nested in a coarse global ocean model (GLB), and four-dimensional variational ocean data assimilation (NPR-4DVAR; Usui et al., 2015) is carried out for the NPR model. The prediction part comprises a fine-resolution (approx. 2 km) ocean model for the area around Japan (JPN) nested in an eddy-resolving North Pacific model (NP) with regular grid spacing that is also two-way nested in the GLB. NPR-4DVAR analysis provides water temperature and salinity data for initialization of the NP and JPN models.

Bias reduction in assimilation of satellite altimetry data and version updating of the forecast models (Sakamoto et al. 2023) were applied to the operational system in February 2023. The bias reduction is reported here.

2. Improvement in satellite altimetry data assimilation

Sea level anomaly (SLA) data derived from satellite altimeters (η_{obs}) incorporate surface dynamic height anomaly (η_{dyn}), barotropic response to surface wind forcing (η_{bt}), changes in total sea water mass over the entire model domain (η_{mass}), and measurement errors. In the JPN system, the η_{dyn} value obtained by subtracting non-steric components (η_{bt} and η_{mass}) from η_{obs} is used for assimilation to determine precise water temperature and salinity. Previously, both η_{bt} and η_{mass} were prescribed as monthly constants based on extrapolation from an ocean reanalysis experiment. To enhance accuracy, the monthly mean non-steric SLA averaged over the model domain is now estimated every day using the latest SLA and in-situ observation data, which is expected to allow more precise analysis of water temperature and salinity. To evaluate this, an experiment employing the updated SLA assimilation scheme (TEST) was conducted, and the results were compared with those from the previous control (CNTL) experiment.

3. Results

The estimated non-steric SLA averaged over GLB largely follows the extrapolated time series, while estimated values for NPR diverge downward from the extrapolation (Figure 1). This implies non-steric SLA overestimation and η_{dyn} underestimation for NPR-4DVAR in CNTL, leading to negative biases in water temperature.

Water temperature biases against in-situ observation in NP subsurface layers at initial states are depicted in Figure 2. The negative biases in CNTL decrease in TEST as expected. Reduced root mean square errors (RMSEs) are also seen in TEST (not shown). Figure 3 compares the biases and RMSEs of CNTL (blue) and TEST (red) averaged over the JPN model domain at initial states. The biases of CNTL are negative for most layers, and the negative biases of TEST are smaller than those of CNTL (Figure 3, top). TEST RMSEs are also smaller than those of CNTL almost everywhere (bottom). Error reduction associated with the smaller bias in the subsurface layer is seen for 10-day forecasts of the NP and JPN models (not shown).

In summary, the improved SLA data assimilation reduces cold biases in subsurface layers for NPR-4DVAR and prediction errors in the NP and JPN models.

References

Hirose, N., N. Usui, K. Sakamoto, H. Tsujino, G. Yamanaka, H. Nakano, S. Urakawa, T. Toyoda, Y. Fujii, and N. Kohno, 2019: Development of a new operational system for monitoring and forecasting coastal and open-ocean states around Japan. Ocean Dyn, 69, 1333–1357.

Sakamoto, K., H. Tsujino, H. Nakano, S. Urakawa, T. Toyoda, N. Hirose, N. Usui, and G. Yamanaka, 2019: Development of a 2-km resolution ocean model covering the coastal seas around Japan for operational application. Ocean Dyn, 69, 1181–1202.

Sakamoto, K., H. Nakano, S. Urakawa, T. Toyoda, Y. Kawakami, H. Tsujino, and G. Yamanaka, 2023: Reference manual for the Meteorological Research Institute Community Ocean Model version 5 (MRI.COMv5). Technical Reports of the Meteorological Research Institute 87, Meteorological Research Institute of Japan Meteorological Agency, Ibaraki, Japan. 334pp. (https://www.mri-jma.go.jp/Publish/Technical/DATA/VOL_87/).

Usui, N., Y. Fujii, K. Sakamoto, and M. Kamachi, 2015: Development of a four-dimensional variational assimilation system for coastal data assimilation around Japan. Mon. Wea. Rev., 143, 3874–3892.

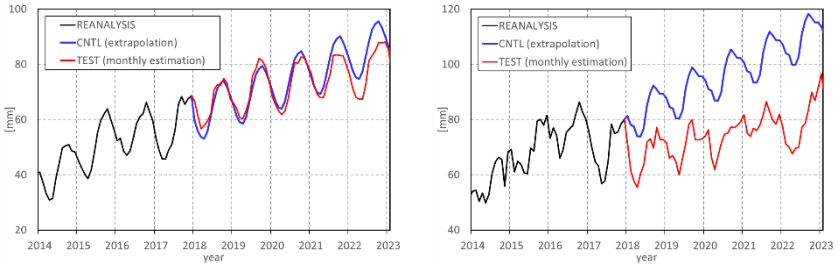

Figure 1 Monthly non-steric SLA averaged over the entire model domain (left: GLB; right: NPR). Black and red lines: monthly estimation; blue lines: extrapolation from black lines.

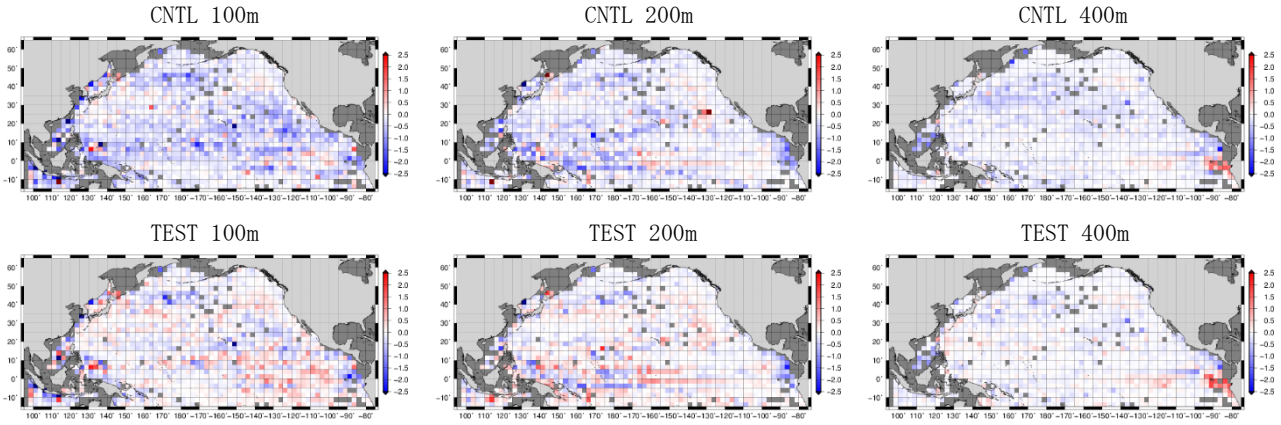

Figure 2 Water temperature biases (model variable minus in-situ observation) at 100 m (left), 200 m (center) and 400 m (right) at NP initial states. Daily observation data are compared with the nearest model grid point value, and biases are averaged within every $2.5^\circ \times 2.5^\circ$ mesh. The verification period is July 2021 – May 2022. The top and bottom panels depict the biases of CNTL and TEST, respectively.

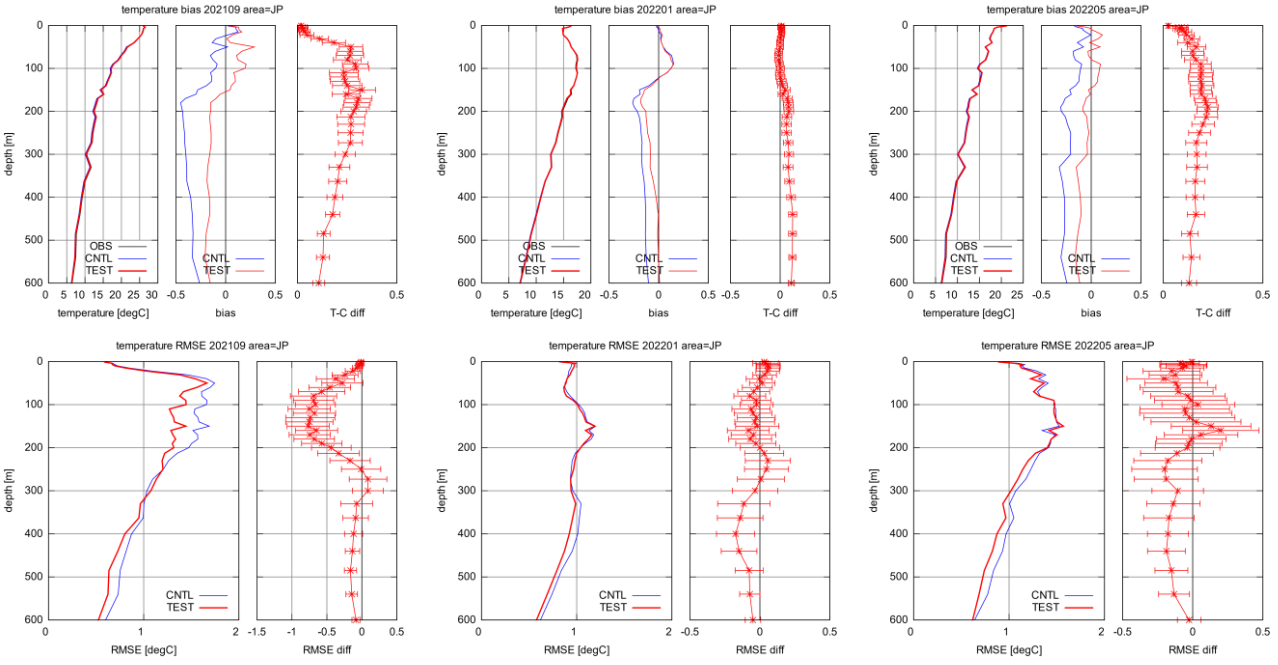

Figure 3 Vertical profiles of bias (top) and RMSE (bottom) for water temperature over the JPN model domain ($117 - 160^\circ\mathrm{E}, 20 - 52^\circ\mathrm{N}$) at initial states for September 2021, January 2022 and May 2022. Top left: in-situ observation (black), CNTL (blue) and TEST (red); top center: CNTL and TEST biases; right: TEST – CNTL. Bottom left: CNTL and TEST RMSEs; right: TEST – CNTL. TEST – CNTL error bars denote a confidence level of 95%.

Ocean Color Data Assimilation and Coupled Ocean Physical-biogeochemical Reanalysis Efforts at NOAA/NCEP

Xiao Liu[1], Avichal Mehra[1], Guillaume Vernieres[1], Daryl Kleist[1], Hae-Cheol Kim[1], Eric Bayler[2], Travis Sluka[3], and Shastri Paturi[1]

[1]NOAA/NWS/NCEP/EMC, College Park, Maryland, USA
[2]NOAA/NESDIS/STAR, College Park, Maryland, USA
[3]JCSDA, Boulder, CO, USA
e-mail: Xiao.Liu@noaa.gov

Ocean biogeochemical processes provide important geophysical feedback to the weather and climate systems through complex ocean biophysical and air-sea interactions. In recent years, multi-platform satellite observations provide nearly global coverage of surface ocean color with repeating daily cycles, enabling the assimilation of near real-time ocean color products (e.g. Chl-a, POC, Kd) in operational ocean forecast systems. This report describes the methodology and techniques used in the implementation of JEDI-based assimilation of multi-source ocean color products in NOAA/NCEP's Unified Forecast System (UFS) - a preoperational, fully coupled Earth modeling and prediction system. We conducted a suite of multi-year ocean analysis experiments with this system, and evaluated the impact of ocean color data assimilation on ocean state predictions with a particular focus on skills at timescales of weeks to months. This work is in support of NOAA/NCEP's subseasonal to seasonal prediction project.

1. JEDI-based ocean color data assimilation

Ocean color data assimilation efforts at NOAA/NCEP leverage the development of [1]SOCA application of [2]JEDI led by [3]JCSDA, with contributions from NOAA/NCEP and other JCSDA partners. Data streams for the Level-2 and Level-3 NOAA-20/VIIRS, S-NPP/VIIRS, and Aqua/MODIS near real-time ocean color observations, as well as for the Level-4 daily VIIRS+OLCI multi-sensor gap-filled chlorophyll (*chlor_a*) analysis, were established from the providers (e.g., NOAA CoastWatch) to NOAA's [4]RDHPCS (e.g., machine "Hera" and "Gaea"). The required software to preprocess ocean color products for first-step quality control and ingestion by the JEDI system was developed to assimilate these observations in a six-tracer biogeochemistry model [5]BLING (Dunne *et al.*, 2020) coupled to [6]MOM6 (Adcroft *et al.*, 2019), which was implemented as the global ocean component in the UFS.

2. Coupled ocean physical-biogeochemical reanalysis

The coupled ocean physical-biogeochemical reanalysis described in this report uses recently released versions of the UFS (*Prototype-8*, DATM application at 0.25° horizontal resolution) and the SOCA model interface to the JEDI system. The variational method (3DVAR) uses the [7]BUMP covariance training libraries provided within the [8]SABER component of the JEDI system. The assimilated ocean color observations in this suite of experiments included S-NPP/VIIRS (NOAA CoastWatch), NOAA-20/VIIRS (OB.DAAC), and Aqua/MODIS (OB.DAAC) Level-3 *chlor_a* products, as well as the Level-4 gap-filled *chlor_a* analysis product (DINEOF, NOAA CoastWatch) described in Section 1. The coupled ocean reanalysis was run for a 2-year period from January 1, 2019 through December 31, 2020. [9]GEFSRR was used as the retrospective atmospheric forcing for Year 2019, which was then replaced by [10]CFSR for Year 2020. Results show that the coupled ocean physical-biogeochemical reanalysis had lower SST prediction errors at a global scale than the ocean physical-only reanalysis (*Figure 1*).

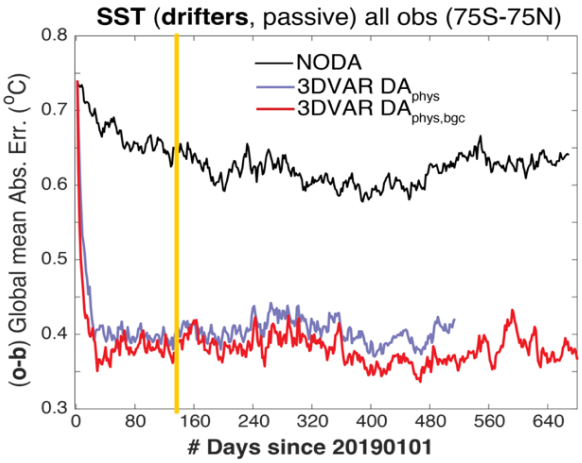

Figure 1. A comparison of the global mean absolute SST prediction errors (observation minus model background, or **o-b**) between two experiments (DA_{phys}: ocean physical-only reanalysis, purple line; $DA_{phys,bgc}$: ocean physical-biogeochemical reanalysis, red line) when compared against independent drifter measurements. Results show that the ocean physical-biogeochemical reanalysis generally had lower SST prediction errors. The yellow line shows the date on which the fully coupled UFS *p8* was initialized after random ensemble perturbations (May 16, 2019).

3. Impact of ocean biogeochemical modeling and data assimilation on SST predictions

To assess the impact of ocean biogeochemical modeling and ocean color data assimilation on the prediction skills of the UFS, we initialized a 12-member ensemble of the fully coupled UFS (with the BLING biogeochemical model enabled) reforecast experiments from the coupled ocean physical-biogeochemical reanalysis on May 16, 2019 after adding small perturbations to each ensemble member's initial model analysis states, and monitored the prediction errors of [11]SST out to 31 days in the fully coupled UFS. We compared the ensemble mean performance of this UFS reforecast system ($UFS_{phys,bgc}$), where ocean biogeochemical modeling and ocean color data assimilation were enabled, against the reference system (UFS_{phys}), where only ocean physics were assimilated and simulated. Results showed that initializing UFS *p8* (with BLING enabled) from the ocean reanalysis system, where ocean color observations were assimilated, resulted in a globally averaged reduction of 4.6% in SST prediction error with a regional reduction of up to 18% for subseasonal time scales (i.e., Weeks 2-4; *Figs. 2,3*). The improvement in SST prediction skills was particularly noticeable during Week 3 and Week 4 of the reforecast period (*Fig. 2*)

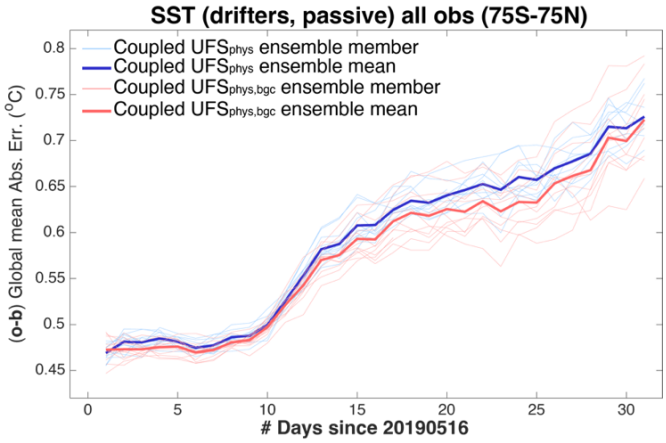

Figure 2. A comparison of the global mean absolute SST prediction errors (**o-b**) between two UFS reforecast experiments when compared against drifter measurements. The impact of ocean color data assimilation and ocean biogeochemical modeling on UFS's SST prediction skills out to 31 days was evaluated where 1) monthly climatological *chlor_a* (blue lines, UFS_{phys}) or 2) BLING simulated *chlor_a* concentration (red lines, $UFS_{phys,bgc}$) was used in UFS's MOM6 opacity routine. Results show that SST prediction errors were lower after two weeks when the BLING model was included in the UFS reforecasts and properly initialized with ocean biogeochemical analysis.

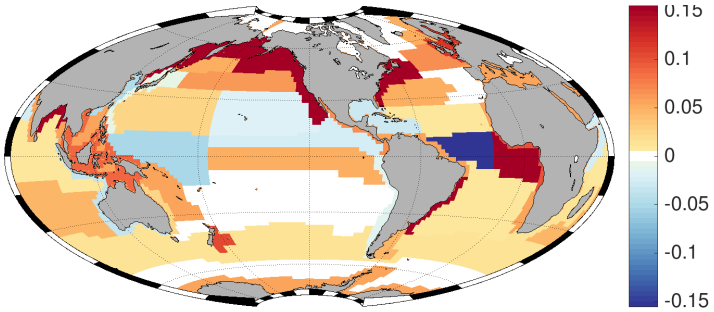

Figure 3. Mean regional difference in SST prediction errors (o-b) between the two UFS reforecast experiments UFS_{phys} and $UFS_{phys,bgc}$, as shown in *Fig. 2*, averaged over Weeks 2-4. Warm, red color indicates improvement in SST prediction skills after enabling ocean data assimilation and ocean biogeochemical modelling, while cool, blue color indicates skill deterioration. The global ocean is separated into 56 provinces for statistical analyses according to Longhurst (2007).

Abbreviations:

[1]SOCA: Sea-ice Ocean Coupled Assimilation
[2]JEDI: Joint Effort for Data Assimilation Integration (JEDI)
[3]JCSDA: Joint Center for Satellite Data Assimilation
[4]RDHPCS: Research and Development High-Performance Computing System
[5]BLING: Biogeochemistry with Light, Iron, Nutrients and Gas
[6]MOM6: Modular Ocean Model version 6
[7]BUMP: Background error on an Unstructured Mesh Package
[8]SABER: System Agnostic Background Error Representation
[9]GEFSRR: The Global Ensemble Forecast System Reforecasting and Reanalysis
[10]CFSR: Climate Forecast System Reanalysis
[11]SST: Sea Surface Temperature

Key references:

Adcroft, A., Anderson, W., Balaji, et al. (2019). The GFDL global ocean and sea ice model OM4.0: Model description and simulation features. *Journal of Advances in Modeling Earth Systems*, 11, 3167– 3211.

Dunne, John P., I Bociu, Benjamin Bronselaer, et al. (2020). Simple Global Ocean Biogeochemistry with Light, Iron, Nutrients and Gas version 2 (BLINGv2): Model description and simulation characteristics in GFDL's CM4.0. *Journal of Advances in Modeling Earth Systems*. DOI:10.1029/2019MS002008.

Longhurst, A. (2007), Ecological Geography of the Sea, Academic Press, London.

Complex System of the Wind Waves Forecasting in the World Ocean and the Seas of Russia

A. A. Zelenko and Yu. D. Resnyanskii

Hydrometeorological Research Center of the Russian Federation, Bolshoi Predtechensky per. 13, Moscow 123376, Russia

Email: zelenko@mecom.ru

Information on the today's and future state of the sea surface, which is almost always disturbed to some extent by wind waves, is one of the most requested by numerous users of marine hydrometeorological information (navigation, rescue operations, marine fishing, obtaining mineral resources, environmental applications, and many others). The usual way for obtaining this kind of information are operational wind waves forecasting systems.

For the purposes of such forecasting in the Hydrometeorological Center of Russia an integrated system is being developed. The system is configured according to the conjugate scheme "ocean – sea – coastal zone" within the framework of a unified technology, taking into account differences in the spatio-temporal scales of wave processes in oceanic and marine areas. Conjugation is accomplished by continuously exchanging information between different subdomains at the liquid boundaries of nested meshes. The system makes it possible to calculate wave parameters with a resolution of 10–20 km in the World Ocean and ~5 km in the Russian seas with a computing time acceptable for operational applications.

The third generation spectral wave model WaveWatch III (WW3) version 6.07 (WW3DG, 2019) is used for computing the forecasts. The model, which is one of the three most known in forecasting applications (WAM, WW3, SWAN), is based on the numerical solution of the spectral equation of the wave energy balance or wave action.

For the global ocean, the computational domain is constructed by combining a regular geographic grid at low and mid latitudes with near polar grids with a resolution close to the resolution of the geographic grid at its boundaries (Table 1). The combination of such grids is carried out using the IRI (irregular – regular – irregular) technology (Rogers and Linzell, 2018), which provides a relatively uniform spatial resolution (10–20 km) for the entire global area. Unlike the usual geographic grid over the entire global region, this configuration does not violate the grid isotropy at high latitudes.

Table 1. Composite grid configurations for the joint calculation of wind waves in the World Ocean

Grid ID	Grid type	Latitude range	Resolution	Number of nautical grid points
nps10km	stereographic	60° – 89° N	~10 km	152822
reg12mn	geographic	55° S – 65° N	0,2° (~20 km)	754030
sps15km	stereographic	50° – 80° S	~15 km	205425

For the marginal seas, grid configurations with a higher spatial are used (Table 2). The lateral boundary conditions for these grids are generated in the course of solving the task for the global domain (Table 2).

Detailing forecasts in the coastal zone (bays, straits, port waters, etc.) requires an even higher resolution, up to ~100 m. This problem is solved by using conjugated unstructured (triangular) grids supported by the WW3 model. Use of this way allows the grid structure to be adapted to the bathymetry and coastline configuration. The boundary conditions for such grids are generated by a submodel for the corresponding sea (Table 2) within the framework of the general scheme "sea–coastal zone".

Table 2. Grid configurations for wind waves forecasting in the Russian seas

Region	Grid ID	Grid type	Resolution	Boundary conditions from the mesh	5 day forecast computing time (min)
Arctic Seas	*arc*	stereographic	~5 km	*reg12mn*	20
White Sea	*bel*	geographic	~1 km	*nps10km*	12
Baltic Sea	*balt*	geographic	~2 km	*reg12mn*	10
Bering Sea	*bering*	geographic	~5 km	*reg12mn*	6
Japan and Okhotsk Seas	*JapOhot*	geographic	~5 km	*reg12mn*	6
Black Sea, Sea of Azov, Kerch Strait.	*black* *azov* *kerch*	geographic geographic geographic	~4 km ~1 km ~0,5 km	— — —	15
Caspian Sea, Northern Caspian	*casp* *caspn*	geographic geographic	~2 km ~1 km	— —	18

For setting boundary conditions on the sea surface, which are required for the wave model integration, the products of two global meteorological forecasting models, PLAV (Hydrometeorological Center of Russia) (Tolstykh et al., 2019) and GFS (NCEP/NOAA), as well as of the national mesoscale forecasting system COSMO-Ru (Rivin et al., 2019) are used.

When using 574 computing cores, the calculations of the global wave forecast for 5 days in the configuration of Table 1 take approximately 18 minutes, and under the conditions of parallel calculation of forecasts for the seas (Table 2), the total time spent is about 40 minutes, which is acceptable for operational applications. Starting from November 1, 2022, the technology operates in an experimental quasi-operational mode.

References

Rivin G. S., Rozinkina I. A., Astakhova E. D., Blinov D. V., Bundel' A. Yu., Kirsanov A. A., Shatunova M. V., Chubarova N. Ye., Alferov D. Yu., Varentsov M. I., Zakharchenko D. I., Kopeykin V. V., Nikitin M. A., Poliukhov A. A., Revokatova A. P., Tatarinovich E. V., Churiulin E. V., 2019: COSMO-Ru high-resolution short-range numerical weather prediction system: Its development and applications. *Hydrometeorological Research and Forecasting*, No. 4 (374). P. 37–54 (in Russian).

Rogers W. E. and Linzell R. S., 2018: The IRI grid system for use with WAVE-WATCH III® (Tech. Rep.). Stennis Space Center, MS 39529-5004: Naval Re1486 search Laboratory.

Tolstykh M.A., Fadeev R.Yu., Shashkin V.V., Travova (Makhnorylova) S.V., Goyman G.S., Mizyak V.G., Rogutov V.S., Shlyaeva A.V., Yurova A.Yu. Development of SL-AV global semi-Lagrangian atmosphere model in 2009–2019, 2019: *Hydrometeorological Research and Forecasting*, No. 4 (374), P. 77–91 (in Russian).

WW3DG (The WAVEWATCH III® Development Group), 2019: User manual and system documentation of WAVEWATCH III® version 6.07. Tech. Note 333, NOAA/NWS/NCEP/MMAB, College Park, MD, USA, 326 pp.